

# Nonlinear PDEs and Numerical Algorithms for Modeling Levelings and Reconstruction Filters

Petros Maragos<sup>1</sup> and Fernand Meyer<sup>2</sup>

<sup>1</sup> National Technical University of Athens, Dept. of Electrical & Computer Engineering, Zografou 15773, Athens, Greece. Email: [maragos@cs.ntua.gr](mailto:maragos@cs.ntua.gr)

<sup>2</sup> Centre de Morphologie Mathématique, Ecole des Mines de Paris, 35, Rue Saint Honoré, 77305 Fontainebleau, France. Email: [meyer@cmm.ensmp.fr](mailto:meyer@cmm.ensmp.fr)

**Abstract.** In this paper we develop partial differential equations (PDEs) that model the generation of a large class of morphological filters, the levelings and the openings/closings by reconstruction. These types of filters are very useful in numerous image analysis and vision tasks ranging from enhancement, to geometric feature detection, to segmentation. The developed PDEs are nonlinear functions of the first spatial derivatives and model these nonlinear filters as the limit of a controlled growth starting from an initial seed signal. This growth is of the multiscale dilation or erosion type and the controlling mechanism is a switch that reverses the growth when the difference between the current evolution and a reference signal switches signs. We discuss theoretical aspects of these PDEs, propose discrete algorithms for their numerical solution and corresponding filter implementation, and provide insights via several experiments. Finally, we outline the use of these PDEs for improving the Gaussian scale-space by using the latter as initial seed to generate multiscale levelings that have a superior preservation of image edges and boundaries.

## 1 Introduction

For several tasks in computer vision, especially the ones related to scale-space image analysis, there have been proposed continuous models based on partial differential equations (PDEs). Motivations for using PDEs include better and more intuitive mathematical modeling, connections with physics, and better approximation to the Euclidean geometry of the problem. While many such continuous approaches have been linear (the most notable example being the isotropic heat diffusion PDE for modeling the Gaussian scale-space), many among the most useful ones are nonlinear. This is partly due to a general understanding about the limitations or inability of linear systems to successfully model several important vision problems.

Areas where there is a need to develop nonlinear approaches include the class of problems related to scale-space analysis and multiscale image smoothing. In contrast to the shifting and blurring of image edges caused by linear smoothers, there is a large variety of nonlinear smoothers that either suffer less

from or completely avoid these shortcomings. Simple examples are the classic morphological openings and closings (cascades of erosions and dilations) as well as the median filters. The openings suppress signals peaks, the closings eliminate valleys, whereas the medians have a more symmetric behavior. All three filter types preserve well vertical image edges but may shift and blur horizontal edges/boundaries. A much more powerful class of filters are the *reconstruction* openings and closings which, starting from a *reference* signal  $f$  consisting of several parts and a *marker* (initial seed)  $g$  inside some of these parts, can reconstruct whole objects with exact preservation of their boundaries and edges. In this reconstruction process they simplify the original image by completely eliminating smaller objects inside which the marker cannot fit. The reconstruction filters enlarge the flat zones of the image [15]. One of their disadvantages is that they treat asymmetrically the image foreground and background. A recent solution to this asymmetry problem came from the development of a more general powerful class of morphological filters, the levelings [10,11], which include as special cases the reconstruction openings and closings. They are transformations  $\Psi(f, g)$  that depend on two signals, the reference  $f$  and the marker  $g$ . Reconstruction filters and levelings have found numerous applications in a large variety of problems involving image enhancement and simplification, geometric feature detection, and segmentation. They also possess many useful algebraic and scale-space properties, discussed in a companion paper [12].

In this paper we develop PDEs that can model and generate levelings. These PDEs work by growing a marker (initial seed) signal  $g$  in a way that the growth extent is controlled by a reference signal  $f$  and its type (expansion or shrinking growth) is switched by the sign of the difference between  $f$  and the current evolution. This growth is modeled by PDEs that can generate multiscale dilations or erosions. Therefore, we start first with a background section on dilation PDEs. Afterwards, we introduce a PDE for levelings of 1D signals and a PDE for levelings of 2D images, propose discrete numerical algorithms for their implementation, and provide insights via experiments. We also discuss how to obtain reconstruction openings and closings from the general leveling PDE. Further, we develop alternative PDEs for modeling generalized levelings that create quasi-flat zones. Finally, we outline the use of these PDEs for improving the Gaussian scale-space by using the latter as initial seed to generate multiscale levelings that have a superior preservation of image edges and boundaries.

## 2 Dilation/Erosion PDEs

All multiscale morphological operations, at their most basic level, are generated by multiscale dilations and erosions, which are obtained by replacing in the standard dilations/erosions the unit-scale kernel (structuring element)  $K(x, y)$  with a multiscale version  $K^{(t)}(x, y) \equiv tK(x/t, y/t)$ ,  $t > 0$ . The *multiscale dilation* of a 2D signal  $f(x, y)$  by  $K^{(t)}$  is the space-scale function

$$\delta(x, y, t) \equiv (f \oplus K^{(t)})(x, y) = \sup_{(a,b)} \{f(x-a, y-b) + tK(a/t, b/t)\}, \quad t > 0$$

where  $\delta(x, y, 0) = f(x, y)$ . Similarly, the multiscale erosion of  $f$  is defined as

$$\varepsilon(x, y, t) \equiv (f \ominus K^{(t)})(x, y) = \inf_{(a,b)} \{f(x + a, y + b) - tK(a/t, b/t)\}$$

Until recently the vast majority of implementations of multiscale morphological filtering had been discrete. In 1992, three teams of researchers independently published nonlinear PDEs that model the continuous multiscale morphological scale-space. In [1] PDEs were obtained for multiscale flat dilation and erosion by compact convex sets as part of a general work on developing PDE-based models for multiscale image processing that satisfy certain axiomatic principles. In [4] PDEs were developed that model multiscale dilation, erosion, opening and closing by compact-support convex sets or concave functions which may have non-smooth boundaries or graphs, respectively. This work was based on the semigroup structure of the multiscale dilation and erosion operators and the use of sup/inf derivatives to deal with the development of shocks. In [18] PDEs were obtained by studying the propagation of boundaries of 2D sets or signal graphs under multiscale dilation and erosion, provided that these boundaries contain no linear segments, are smooth and possess a unique normal at each point. Refinements of the above three works for PDEs modeling multiscale morphology followed in [2,5,6,8,9,19]. The basic dilation PDE was applied in [3,16] for modeling continuous-scale morphology, where its superior performance over discrete morphology was noted in terms of isotropy and subpixel accuracy. Next we provide a few examples.<sup>1</sup>

For 1D signals  $f(x)$ , and if  $K(x)$  is the  $0/ - \infty$  indicator function of the interval  $[-1, 1]$ , then the PDEs generating the multiscale flat dilation  $\delta(x, t)$  and erosion  $\varepsilon(x, t)$  of  $f$  are:

$$\delta_t = |\delta_x| \quad , \quad \varepsilon_t = -|\varepsilon_x| \tag{1}$$

with initial values  $\delta(x, 0) = \varepsilon(x, 0) = f(x)$ .

For 2D signals  $f(x, y)$ , and if  $K(x, y)$  is the  $0/ - \infty$  indicator function of the unit disk, then the PDEs generating the multiscale flat dilation  $\delta(x, y, t)$  and erosion  $\varepsilon(x, y, t)$  of  $f$  are:

$$\delta_t = \|\nabla\delta\| = \sqrt{(\delta_x)^2 + (\delta_y)^2}; \quad , \quad \varepsilon_t = -\|\nabla\varepsilon\| \tag{2}$$

with initial values  $\delta(x, y, 0) = \varepsilon(x, y, 0) = f(x, y)$ .

These simple but nonlinear PDEs are satisfied at points where the data are smooth, i.e., the partial derivatives exist. However, even if the initial image/signal  $f$  is smooth, at finite scales  $t > 0$  the above multiscale dilation evolution may create discontinuities in the derivatives of  $\delta$ , called *shocks*, which then continue propagating in scale-space. Thus, the multiscale dilations are *weak solutions* of the corresponding PDEs.

The above PDEs for dilations of graylevel images by flat structuring elements directly apply to binary images, because flat dilations commute with thresholding and hence, when the graylevel image is dilated, each one of its thresholded

<sup>1</sup> Notation: For  $u = u(x, y, t)$ ,  $u_t = \partial u / \partial t$ ,  $u_x = \partial u / \partial x$ ,  $u_y = \partial u / \partial y$ ,  $\nabla u = (u_x, u_y)$ .

versions representing a binary image is simultaneously dilated by the same element and at the same scale. However, this is not the case with graylevel structuring functions. For example, if  $K(x, y) = -a(x^2 + y^2)$ ,  $a > 0$ , is an infinite-support parabolic function, the dilation PDE becomes

$$\delta_t = \|\nabla\delta\|^2/4a = [(\delta_x)^2 + (\delta_y)^2]/4a \tag{3}$$

### 3 PDE for 1D Leveling

Consider a 1D signal  $f(x)$  and a marker signal  $g(x)$  from which a leveling  $\Psi(f, g)$  will be produced.

If  $g \leq f$  everywhere and we start iteratively growing  $g$  via incremental flat dilations with an infinitesimally small element  $[-\Delta t, \Delta t]$  but without ever growing the result above the graph of  $f$ , then in the limit we shall have produced the *opening by reconstruction* of  $f$  (with respect to the marker  $g$ ), which is a special leveling. The infinitesimal generator of this signal evolution can be modeled via a dilation PDE that has a mechanism to stop the growth whenever the intermediate result attempts to create a function larger than  $f$ . Specifically, let  $u(x, t)$  represent the evolutions of  $f$  with initial value  $u_0(x) = u(x, 0) = g(x)$ . Then,  $u$  is a weak solution of the following initial-value PDE system

$$u_t = \text{sign}(f - u)|u_x| = \begin{cases} |u_x|, & u < f \\ 0, & u = f \text{ or } u_x = 0 \end{cases} \tag{4}$$

$$u(x, 0) = g(x) \leq f(x) \tag{5}$$

where  $\text{sign}(r)$  is equal to  $+1$  if  $r > 0$ ,  $-1$  if  $r < 0$  and  $0$  if  $r = 0$ . This PDE models a *conditional dilation* that grows the intermediate result as long as it does not exceed  $f$ . In the limit we obtain the final result  $u_\infty(x) = \lim_{t \rightarrow \infty} u(x, t)$ . The mapping  $u_0 \mapsto u_\infty$  is the *opening by reconstruction filter*.

If in the above paradigm we reverse the order between  $f$  and  $g$ , i.e., assume that  $g(x) \geq f(x) \forall x$ , and replace the positive growth (dilation) of  $g$  with negative growth via erosion that stops when the intermediate result attempts to become smaller than  $f$ , then we obtain the *closing by reconstruction* of  $f$  with respect to the marker  $g$ . This is another special case of a leveling, whose generation can be modeled by the following PDE:

$$u_t = -\text{sign}(u - f)|u_x| = \begin{cases} -|u_x|, & u > f \\ 0, & u = f \text{ or } u_x = 0 \end{cases} \tag{6}$$

$$u(x, 0) = g(x) \geq f(x) \tag{7}$$

What happens if we use any of the above two PDEs when there is no specific order between  $f$  and  $g$ ? The signal evolutions are stored in a function  $u(x, t)$  that is a weak solution of the initial-value PDE system

$$\begin{aligned} u_t(x, t) &= |u_x(x, t)|\text{sign}[f(x) - u(x, t)] \\ u(x, 0) &= g(x) \end{aligned} \tag{8}$$

This PDE has a varying coefficient  $\text{sign}(f - u)$  with spatio-temporal dependence which controls the instantaneous growth and stops it whenever  $f = u$ . (Of course, there is no growth also at extrema where  $u_x = 0$ .) The control mechanism is of a switching type: For each  $t$ , at points  $x$  where  $u(x, t) < f(x)$  it acts as a dilation PDE and hence shifts parts of the graph of  $u(x, t)$  with positive (negative) slope to the left (right) but does not move the extrema points. Wherever  $u(x, t) > f(x)$  the PDE acts as an erosion PDE and reverses the direction of propagation. The final result  $u_\infty(x) = \lim_{t \rightarrow \infty} u(x, t)$  is a general *leveling* of  $f$  with respect to  $g$ . We call (8) a *switched dilation* PDE. The switching action of this PDE model occurs at zero crossings of  $f - u$  where shocks are developed. Obviously, the PDEs generating the opening and closing by reconstruction are special cases where  $g \leq f$  and  $g \geq f$ , respectively. However, the PDEs generating the reconstruction filters do not involve switching of growth.

The switching between a dilation- or erosion-type PDE also occurs in a class of nonlinear time-dependent PDEs which was proposed in [13] to deblur images and/or enhance their contrast by generating shocks and hence sharpening edges. For 1D images a special case of such a PDE is

$$u_t = -|u_x| \text{sign}(u_{xx}) \tag{9}$$

A major conceptual difference between the above edge-sharpening PDE and our PDE generating levelings is that in the former the switching is determined by the edges, i.e., the inflection points of  $u$  itself whereas in the latter the switching is controlled by comparing  $u$  against the reference signal  $f$ . Note also that, if at some point there is an edge in the leveling output, then there must exist an edge of equal or bigger size in the initial (reference) image.

### 3.1 Discretization, Algorithm, Experiments

To produce a shock-capturing and entropy-satisfying numerical method for solving the general leveling PDE (8), we use ideas from the technology of solving PDEs corresponding to hyperbolic conservation laws [7] and Hamilton-Jacobi formulations [14]. Thus, we propose the following discretization scheme, which is an adaptation of a scheme proposed in [13] for solving (9).

Let  $U_i^n$  be the approximation of  $u(x, t)$  on a grid  $(i\Delta x, n\Delta t)$ . Consider the forward and backward difference operators:

$$D_+^x u \equiv \frac{u(x + \Delta x, t) - u(x, t)}{\Delta x}, \quad D_-^x u \equiv \frac{u(x, t) - u(x - \Delta x, t)}{\Delta x} \tag{10}$$

(Similarly we define the difference operators  $D_+^y$  and  $D_-^y$  along the  $y$  direction.) Then we approximate the leveling PDE (8) by the following nonlinear difference equation:

$$U_i^{n+1} = U_i^n - \Delta t [ (S_i^n)^+ \sqrt{((D_-^x U_i^n)^+)^2 + ((D_+^x U_i^n)^-)^2} + (S_i^n)^- \sqrt{((D_+^x U_i^n)^+)^2 + ((D_-^x U_i^n)^-)^2} ] \tag{11}$$

where  $S_i^n = \text{sign}(f(i\Delta x) - U_i^n)$ ,  $r^+ = \max(0, r)$ , and  $r^- = \min(0, r)$ . For stability,  $(\Delta t/\Delta x) \leq 0.5$  is required. Further, at each iteration we enforce the sign consistency

$$\text{sign}(U^n - f) = \text{sign}(g - f) \tag{12}$$

We have not proved theoretically that the above iterated scheme converges when  $n \rightarrow \infty$ , but through many experiments we have observed that it converges in a finite number of steps. Examples are shown in Fig. 1.

### 4 PDE for 2D Leveling

A straightforward extension of the leveling PDE from 1D to 2D signals is to replace the 1D dilation PDE with the PDE generating multiscale dilations by a disk. Then the 2D leveling PDE becomes:

$$\begin{aligned} u_t(x, y, t) &= \|\nabla u(x, y, t)\| \text{sign}[f(x, y) - u(x, y, t)] \\ u(x, y, 0) &= g(x, y) \end{aligned} \tag{13}$$

Of course, we could select any other PDE modeling dilations by shapes other than the disk, but the disk has the advantage of creating an isotropic growth.

For discretization, let  $U_{i,j}^n$  be the approximation of  $u(x, y, t)$  on a computational grid  $(i\Delta x, j\Delta y, n\Delta t)$ . Then we approximate the leveling PDE (13) by the following 2D nonlinear difference equation:

$$\begin{aligned} U_{i,j}^{n+1} &= U_{i,j}^n - \Delta t [\dots \\ & (S_{i,j}^n)^+ \sqrt{((D_-^x U_{i,j}^n)^+)^2 + ((D_+^x U_{i,j}^n)^-)^2 + ((D_-^y U_{i,j}^n)^+)^2 + ((D_+^y U_{i,j}^n)^-)^2} \\ & + (S_{i,j}^n)^- \sqrt{((D_+^x U_{i,j}^n)^+)^2 + ((D_-^x U_{i,j}^n)^-)^2 + ((D_+^y U_{i,j}^n)^+)^2 + ((D_-^y U_{i,j}^n)^-)^2} ] \end{aligned} \tag{14}$$

where  $S_{i,j}^n = \text{sign}(f(i\Delta x, j\Delta y) - U_{i,j}^n)$ . For stability,  $(\Delta t/\Delta x + \Delta t/\Delta y) \leq 0.5$  is required. Also, the sign consistency (12) is enforced at each iteration.

Three examples of the action of the above 2D algorithm are shown in Fig. 2.

## 5 Discussion and Extensions

### 5.1 PDEs for Levelings with Quasi-Flat Zones

So far all the previous leveling PDEs produce filtering outputs that consist of portions of the original (reference) signal and of flat zones (plateaus). Actually they enlarge the flat zones of the reference signal. Is it possible to generate via PDEs generalized levelings that have quasi-flat zones? For example, zones with constant linear slope or zones with parabolic surface? The answer is yes. We illustrate it via the parabolic example. If we replace the flat dilation PDE generator in (8) with the PDE generator for multiscale dilations by a 1D unit-scale parabola  $K(x) = -ax^2$  we obtain the PDE for 1D parabolic levelings:

$$\begin{aligned} u_t(x, t) &= \frac{1}{4a} |u_x(x, t)|^2 \text{sign}[f(x) - u(x, t)] \\ u(x, 0) &= g(x) \end{aligned} \tag{15}$$

To obtain the PDE for 2D parabolic levelings we replace  $|u_x|$  with  $\|\nabla u\|$ .

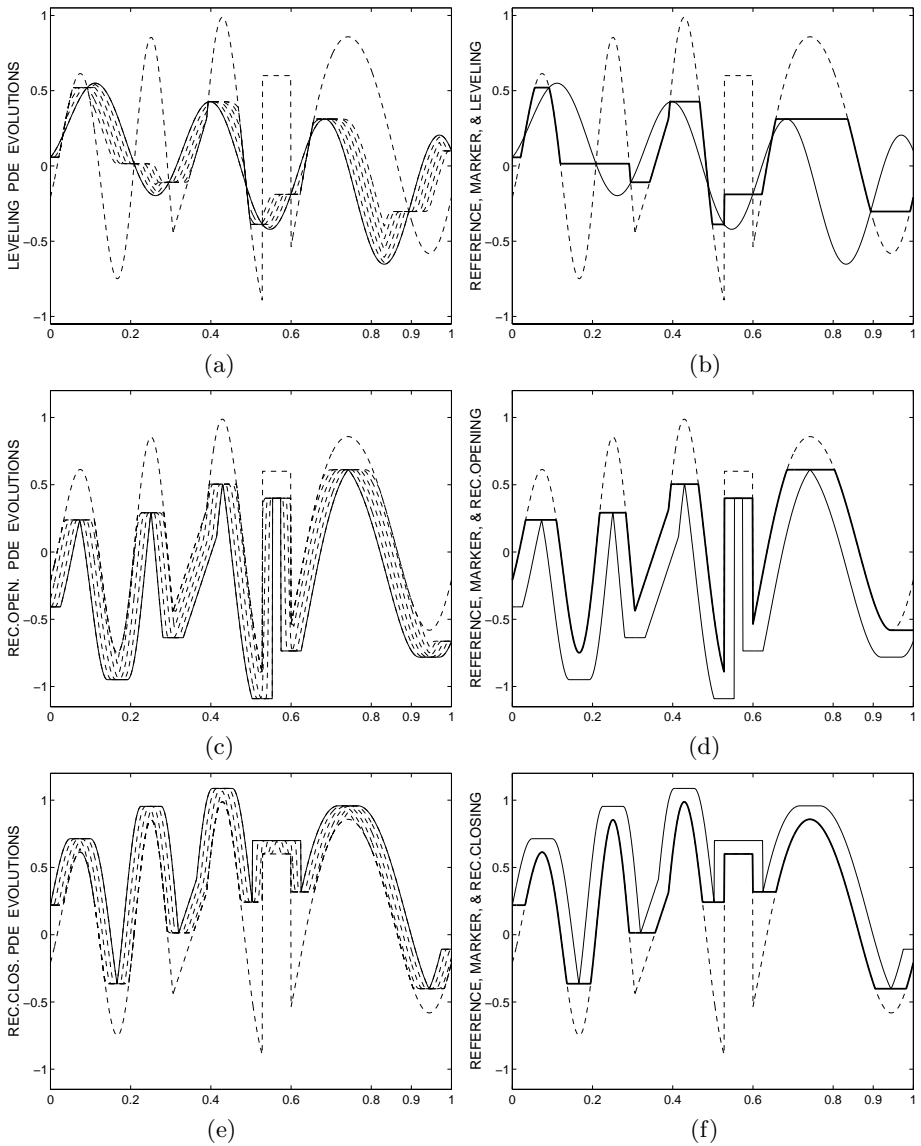


**Fig. 1.** Evolutions of 1D leveling PDE for 3 different markers. For each row, the right column shows the reference signal  $f$  (dash line), the marker (thin solid line), and the leveling (thick solid line). The left column shows the marker and 5 of its evolutions at times  $t = n20\Delta t$ ,  $n = 1, 2, 3, 4, 5$ . In row (a,b) we see the general leveling evolutions for an arbitrary marker. In row (c,d) the marker was an erosion of  $f$  minus a constant, and hence the leveling is a reconstruction opening. In row (e,f) the marker was a dilation of  $f$  plus a constant, and hence the leveling is a reconstruction closing. ( $\Delta x = 0.001$ ,  $\Delta t = 0.0005$ .)

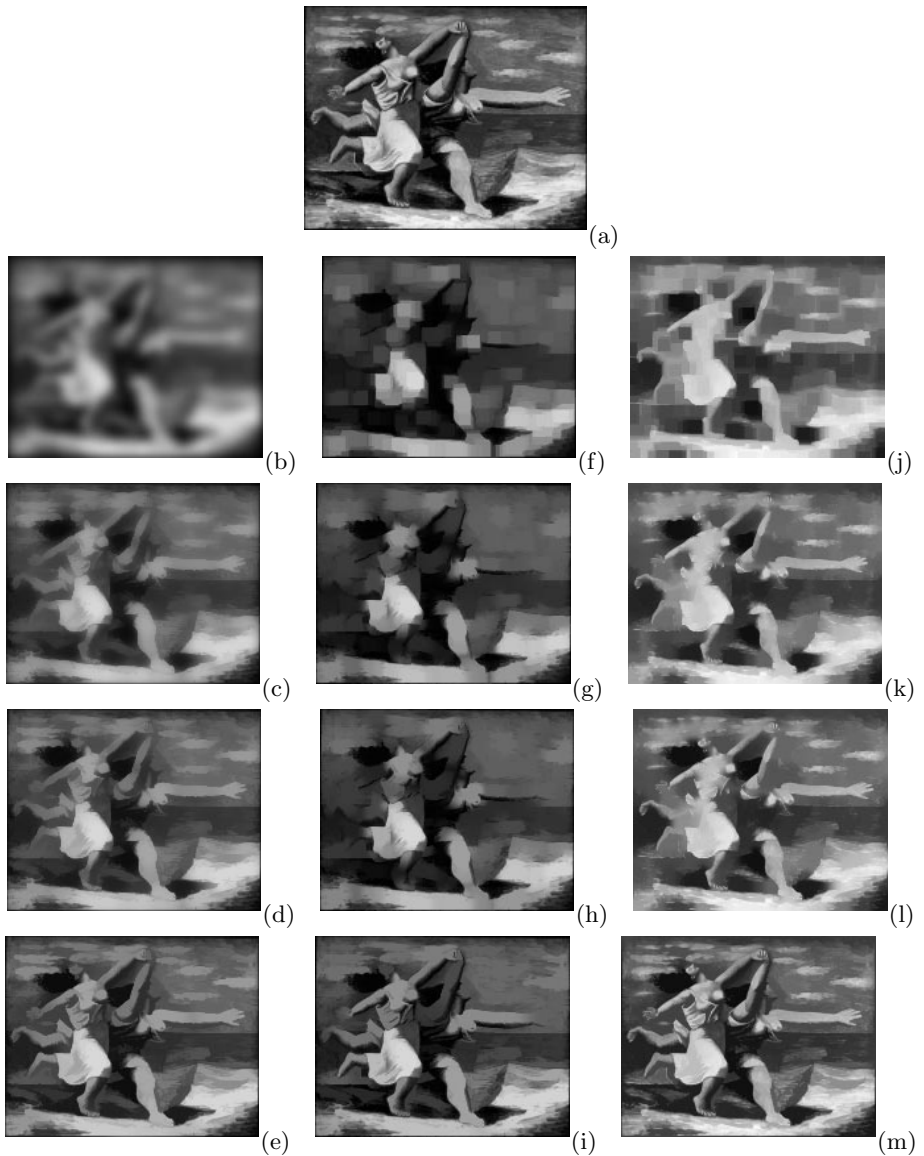


**Fig. 2.** Evolutions of the 2D leveling PDE on the reference top image (a) using 3 markers. Each column shows evolutions from the same marker. On second row the markers ( $t = 0$ ) are shown, on third and fourth rows two evolutions at  $t = 10\Delta t$  and  $t = 20\Delta t$ , and on fifth row the final levelings (after convergence). For left column (b-e), the marker (b) was obtained from a 2D convolution of  $f$  with a Gaussian of  $\sigma = 4$ . For middle column (f-i), the marker (f) was a simple opening by a square of  $9 \times 9$  pixels and hence the corresponding leveling (i) is a reconstruction opening. For right column (j-m), the marker (j) was a simple closing by a square of  $9 \times 9$  pixels and hence the corresponding leveling (m) is a reconstruction closing. ( $\Delta x = \Delta y = 1$ ,  $\Delta t = 0.25$ .)

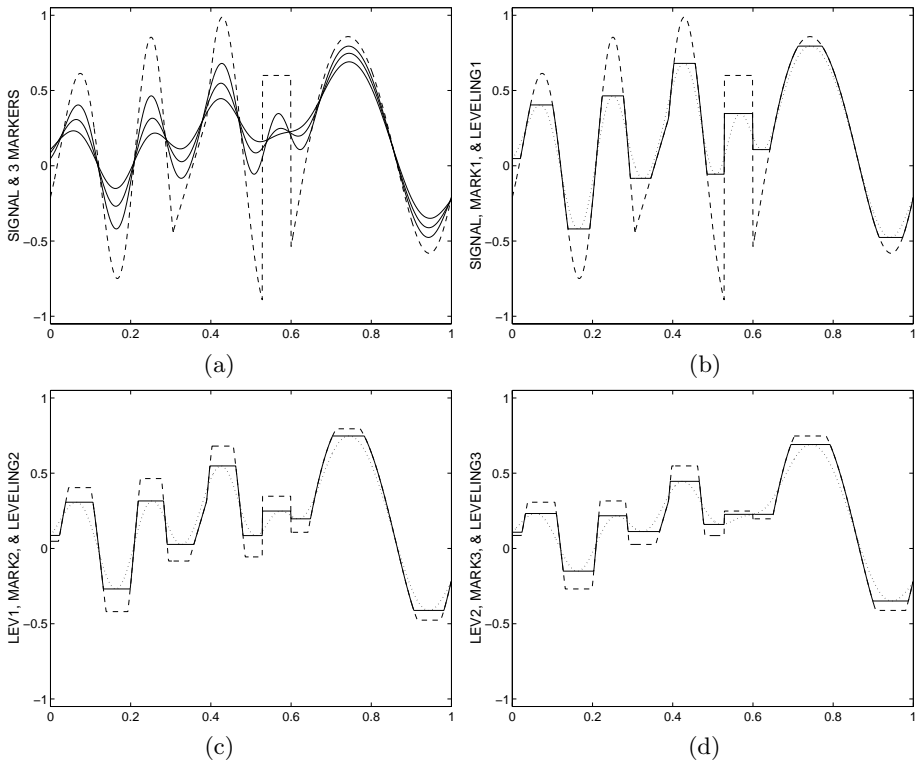


**Fig. 3.** 1D Multiscale levelings. (a) Original (reference) signal  $f$  (dash line) and 3 markers  $g_i$  obtained by convolving  $f$  with Gaussians of standard deviations  $\sigma_i = 30, 40, 50$ . (b)-(d) show reference signals  $g_i$  (dash line), markers  $g_{i+1}$  (dotted line), and levelings  $\Psi(g_i, g_{i+1})$  (solid line) for  $i = 0, 1, 2$ , where  $g_0 = f$ . ( $\Delta x = 0.001$ ,  $\Delta t = 0.0005$ .)



Original Reference



Marker 1



Leveling 1



Marker 2



Leveling 2



Marker 3



Leveling 3

**Fig. 4.** Multiscale image levelings. The markers were obtained by convolving reference image with 2D Gaussians of standard deviations  $\sigma = 3, 5, 7$ . ( $\Delta x = \Delta y = 1$ ,  $\Delta t = 0.25$ .)

## 5.2 Why Use PDEs For Levelings?

In addition to the well-known advantages of the PDE approach (such as more insightful mathematical modeling, more connections with physics, better isotropy, better approximation of Euclidean geometry, and subpixel accuracy), during construction of levelings or reconstruction filters it is possible in some applications to need to stop the marker growth before convergence. In such cases, the isotropy of the partially grown marker offered by the PDE is an advantage. Further, there are no simple digital algorithms for constructing levelings with quasi-flat zones, whereas for the PDE approach only a simple change of the generator is needed.

## 5.3 From Gaussian Scale-Space to Multiscale Levelings

Consider a reference signal  $f$  and a leveling  $\Psi$ . If we can produce various markers  $g_i$ ,  $i = 1, 2, 3, \dots$ , that are related to some increasing scale parameter  $i$  and produce the levelings of  $f$  with respect to these markers, then we can generate multiscale levelings in some approximate sense. This scenario will be endowed with an important property if we slightly change it to the following hierarchy:

$$h_1 = \Psi(f, g_1), h_2 = \Psi(h_1, g_2), h_3 = \Psi(h_2, g_3), \dots \quad (16)$$

The above sequence of steps insures that  $h_j$  is a leveling of  $h_i$  for  $j > i$ .

The sequence of markers  $g_i$  may be obtained from  $f$  in any meaningful way. In this paper we consider the case where the  $g_i$  are multiscale convolutions of  $f$  with Gaussians of increasing standard deviations  $\sigma_i$ . Examples of constructing multiscale levelings from Gaussian convolution markers according to (16) are shown in Fig. 3 for a 1D signal and in Fig. 4 for an image  $f$ . The sequence of the multiscale markers can be viewed as a scale-sampled Gaussian scale-space. As shown in the experiments, the image edges and boundaries which have been blurred and shifted by the Gaussian scale-space are better preserved across scales by the multiscale levelings that use the Gaussian convolutions as markers.

## Acknowledgements

We wish to thank Profs. J. Barrera and R. Lotufo for inviting us to talk at SIBGRAPI'98 in Brazil. The ideas in this paper were formed from our collaboration during this research visit.

P. Maragos' work in this paper was partially supported by the European TMR/Networks Project ERBFMRXCT970160.

## References

1. L. Alvarez, F. Guichard, P.L. Lions, and J.M. Morel, "Axiomatization et nouveaux operateurs de la morphologie mathematique", *C. R. Acad. Sci. Paris*, pp. 265-268, t.315, Serie I, 1992.

2. L. Alvarez, F. Guichard, P.L. Lions, and J.M. Morel, "Axioms and Fundamental Equations of Image Processing", *Archiv. Rat. Mech.*, vol. 123 (3), pp. 199–257, 1993.
3. A. Arehart, L. Vincent and B. Kimia, "Mathematical Morphology: The Hamilton-Jacobi Connection", in *Proc. Int'l Conf. Comp. Vision*, pp. 215–219, 1993.
4. R. W. Brockett and P. Maragos, "Evolution Equations for Continuous-Scale Morphology", *Proc. IEEE Int'l Conf. Acoust., Speech, Signal Processing*, San Francisco, CA, March 1992.
5. R. Brockett and P. Maragos, "Evolution Equations for Continuous-Scale Morphological Filtering", *IEEE Trans. Signal Processing*, vol. 42, pp. 3377–3386, Dec. 1994.
6. H.J.A.M. Heijmans and P. Maragos, "Lattice Calculus and the Morphological Slope Transform", *Signal Processing*, vol. 59, pp. 17–42, 1997.
7. P. D. Lax, *Hyperbolic Systems of Conservation Laws and the Mathematical Theory of Shock Waves*, SIAM, Philadelphia, PA, 1973.
8. P. Maragos, "Differential Morphology and Image Processing" *IEEE Trans. Image Processing*, vol. 78, pp. 922–937, June 1996.
9. P. Maragos and M. A. Butt, "Curve Evolution, Differential Morphology, and Distance Transforms Applied to Multiscale and Eikonal Problems", *Fundamentae Informatica*, to appear.
10. F. Meyer, "From Connected Operators to Levelings", in *Mathematical Morphology and Its Applications to Image and Signal Processing*, H. Heijmans and J. Roerdink, editors, Kluwer Acad. Publ., 1998.
11. F. Meyer, "The Levelings", in *Mathematical Morphology and Its Applications to Image and Signal Processing*, H. Heijmans and J. Roerdink, editors, Kluwer Acad. Publ., 1998.
12. F. Meyer and P. Maragos, "Morphological Scale-Space Representation with Levelings", *Proc. 2nd Int'l. Conf. on Scale-Space Theories in Computer Vision*, Corfu, Greece, Sep. 1999.
13. S. Osher and L. I. Rudin, "Feature-Oriented Image Enhancement Using Schock Filters", *SIAM J. Numer. Anal.*, vol. 27, no. 4, pp. 919–940, Aug. 1990.
14. S. Osher and J. Sethian, "Fronts Propagating with Curvature-Dependent Speed: Algorithms Based on Hamilton-Jacobi Formulations", *J. Comput. Physics*, 79, pp. 12–49, 1988.
15. P. Salembier and J. Serra, "Flat Zones Filtering, Conencted Operators, and Filters by Reconstruction", *IEEE Trans. Image Process.*, vol. 4, pp.1153–1160, Aug. 1995.
16. G. Sapiro, R. Kimmel, D. Shaked, B. Kimia, and A. Bruckstein, "Implementing Continuous-scale Morphology via Curve Evolution", *Pattern Recognition*, 26(9), pp. 1363–1372, 1993.
17. J. A. Sethian, *Level Set Methods*, Cambridge Univ. Press, 1996.
18. R. Van den Boomgaard, *Mathematical Morphology: Extensions towards Computer Vision*, Ph.D. Thesis, Univ. of Amsterdam, The Netherlands, 1992.
19. R. Van den Boomgaard and A. Smeulders, "The Morphological Structure of Images: The Differential Equations of Morphological Scale-Space", *IEEE Trans. Pattern Anal. Mach. Intellig.*, vol. 16, pp.1101–1113, Nov. 1994.